ELSEVIER

Thermochimica Acta 267 (1995) 169–180

thermochimica acta

Pore size distribution measurements of polymer hydrogel membranes for artificial kidneys using differential scanning calorimetry[1]

K. Ishikiriyama[a,*], A. Sakamoto[a], M. Todoki[a], T. Tayama[b], K. Tanaka[b], T. Kobayashi[b]

[a]*Toray Research Center, Inc., Material Characterization Laboratories, 3-7 Sonoyama 3-Chome, Otsu, Shiga 520, Japan*

[b]*Toray Industries, Inc., 3-7 Sonoyama 3-Chome, Otsu, Shiga 520, Japan*

Received 30 November 1994; accepted 22 February 1995

Abstract

The pore size distributions, PSDs, of hydrogel-hollow-fiber membranes such as poly(methyl methacrylate), cellulose triacetate, polyacrylonitrile and polysulfone utilized as artificial kidneys have been characterized using differential scanning calorimetry via thermal porosimetry, termed thermoporosimetry by the authors. The nitrogen gas adsorption-desorption technique was applied to the membranes after freeze-drying to determine the PSDs and, moreover, thermoporosimetry was applied to the membranes before freeze-drying and those refilled with water after freeze-drying, i.e. after nitrogen gas adsorption-desorption measurements. As a result, for the freeze-dried membranes, the PSDs determined using nitrogen gas desorption were found to be generally in good agreement with those obtained using thermoporosimetry. In addition, the PSDs of the poly(methyl methacrylate) membrane before and after freeze-drying were found to be quite different, although the PSDs of the cellulose triacetate, polyacrylonitrile and polysulfone membranes were nearly similar before and after freeze-drying.

Keywords: DSC; Nitrogen gas adsorption-desorption; Pore size distribution; Artificial kidney; Hydrogel; Water

* Corresponding author.

[1] Presented at the 30th Anniversary Conference of the Japan Society of Calorimetry and Thermal Analysis, Osaka, Japan, 31 October–2 November 1994.

0040-6031/95/$09.50 © 1995 – Elsevier Science B.V. All rights reserved
SSDI 0040-6031 (95) 02476-X

1. Introduction

Pore size distribution (PSD) of hydrogel-hollow-fiber membranes utilized as artificial kidneys is one of the predominant factors governing the permeability of water and solute through the membrane; however, it is difficult to characterize the PSDs in the hydrogel-hollow-fiber membranes, because conventional techniques such as mercury porosimetry, gas adsorption-desorption and electron microscopy, which are utilized only for characterizing dry materials, can hardly be applied to pore structure analysis due to irreversible pore collapse and a considerable reduction in the internal porosity.

Homshaw [1] qualitatively clarified, however, the pore structure of never-dried polyacrylonitrile (PAN) hydrogel fibers using differential scanning calorimetry. The PSDs of unheated PAN and heated PAN in water at 100°C for about 2 h were presumed from the freezing and melting temperature depression of water confined in pores. He found that the heated PAN showed a 49% reduction in porosity and that the pore radius of the heated PAN was presumed to be less than that of the unheated PAN; nevertheless, the PSDs were not quantitatively determined because a technique for calculating pore radius from the freezing or melting depression of water had not been established.

In contrast, Eyraud, Brun and Quinson et al. had proposed a methodology to evaluate PSD from the freezing depression of water confined in the pores, and it was applied to many kinds of porous materials [2–10]. Eyraud suggested, however, that the characterization of organic membranes for ultrafiltration, hemodialysis or dialysis prepared by a gelification process followed by coagulation was difficult because the membranes are often asymmetrical and the pore volume of active layer is very small [2].

On the other hand, the authors have recently proposed another new methodology regarding thermal porosimetry, which has been termed thermoporosimetry by the authors, for determining the PSDs from the freezing or melting distribution of freezable pore water using differential scanning calorimetry (DSC) [11]. The methodology was applied to the pore structure analysis of commercially supplied silica gels [12] and of poly(methyl methacrylate) (PMMA) hydrogel-hollow-fiber membranes utilized as artificial kidneys [13]. Hydrodynamic analysis of the PMMA membranes was also carried out, and consequently the average pore radii and the cumulative number of pores obtained using DSC were found to be in good agreement with those hydrodynamically calculated from water permeabilities of the membranes [13].

The present article reports the PSDs of some polymer hydrogel-hollow-fiber membranes utilized as artificial kidneys such as cellulose triacetate (CTA), polyacrylonitrile (PAN) and polysulfone (PS) including PMMA, which were determined using thermoporosimetry and nitrogen gas adsorption-desorption. The nitrogen gas adsorption-desorption measurements of the membranes after freeze-drying were carried out, although thermoporosimetry was carried out with membranes both before and after freeze-drying. For the membranes which were soaked in water again after freeze-drying, the PSDs obtained via nitrogen gas adsorption-desorption are compared with those obtained via thermoporosimetry. In this paper, the changes in the PSDs before and after freeze-drying are also described.

2. Materials and experimental methods

2.2. Samples

Five different hydrogel-hollow-fiber membranes for artificial kidneys were investigated: PMMA (BK-1.6U, Toray), PAN (PAN-17DX, Asahi), PS (PS-1.6UW, Kawasumi), CTA-U (cellulose triacetate, FB-1 70UGA, Nipro) and CTA-E (cellulose triacetate, FB-170EGA, Nipro). The PMMA, CTA-U and CTA-E membranes were homogeneous and symmetrical, while the PAN and PS membranes, which had a closely adherent skin layer on the surface, were asymmetrical.

2.3. Measurements

A sample of about 10–20 mg was hermetically sealed in a high-pressure aluminum crucible that was covered with aluminum oxide on the surface to avoid reaction of water with the aluminum. The freezing and melting curves of the water in the hydrogel-hollow-fiber membranes were determined using a Perkin-Elmer differential scanning calorimeter, DSC-II, equipped with a cooling apparatus and with a data processing system developed by the authors. The DSC measurements for the symmetrical membranes such as PMMA and CTA were performed over a temperature range from 213 to 293 K at a low scanning rate of 0.31 K min^{-1} to avoid thermal and time delays in the DSC curve, and the melting curves were measured to determine the PSDs. On the other hand, for the asymmetric membranes such as PS and PAN, the DSC measurements were performed at a scanning rate of 2.5 K min^{-1} to obtain high sensitivity in the DSC measurements, because the pore volumes in the active layer existing on the surface of the hollow fibers were very small, and the freezing curves were measured to avoid thermal and time delays due to the existence of many large pores. A particular procedure was adopted to obtain the freezing curves without significant supercooling as follows. Firstly, the sample was rapidly precooled to 233 K, and then it was held isothermally at that temperature for more than 10 min. Secondly, the sample was preheated to 272.7 K at a scanning rate of 10 K min^{-1}, and then it was held isothermally at that temperature for more than 10 min. While the sample was subsequently cooled from 272.7 to 233 K at a scanning rate of 2.5 K min^{-1}, the exothermic curves were recorded.

The heat fluxes of the heating and cooling curves were calibrated using the heat of melting of distilled, deionized water purchased from Wako Pure Chemical Industries. Furthermore, the temperature calibration of the heating curve was carried out using the onset temperature of the melting peak of pure water; whereas, the temperature calibration of the cooling curve was carried out by extrapolating the melting onset temperature, which is a function of the scanning rate, to −2.5 K min^{-1}, because it is difficult to calibrate the temperature during cooling using crystallization of a standard sample due to supercooling. When the PSD curves were calculated from the DSC curves, the temperature calibration for correcting thermal and time delays was performed in a way similar to conventional purity analysis using DSC, in which the slope of melting of indium was utilized. The accuracies of the heat flux and the temperature were estimated to be about ±3% or better and about ±0.3 K or better, respectively. At the end of each DSC meas-

urement, a small hole was made in the crucible and then it was dried under vacuum in an oven at 373 K for determining the mass of the water. The transformations of the DSC curves into the PSD curves were carried out using a computer program, written by the authors using the C language, followed by a procedure reported in previous papers [11,12].

For measurements of nitrogen gas adsorption-desorption, a BELSORP 36 system (Nihon Bel) was used for characterizing pore size distributions of the membranes after freeze-drying. The freeze-drying of the membranes was carried out by drying in a vacuum at about 200 K for 2 weeks after quenching from room temperature using liquid nitrogen. After the nitrogen gas adsorption-desorption measurements were performed, the samples were refilled with water, and then the system was maintained under reduced pressure with an aspirator to fill the pores in the membranes with water. Subsequently, the DSC measurements of the samples were carried out to determine the PSDs of the membranes after freeze-drying.

3. Results and discussion

3.1. DSC curves of water in the membranes

Fig. 1 shows the DSC scans of the hydrogel-hollow-fiber membranes for artificial kidneys before freeze-drying. The heating curves of the symmetrical membranes such as CTA-U, CTA-E and PMMA and the cooling curves of the asymmetrical membranes such as PAN and PS are demonstrated. As can been seen from the figure, the freezing or melting temperature depression water was present in all the membranes. There are two viewpoints regarding the water: One is freezable pore water lowering the freezing and melting temperature due to the ice–water interfacial tension [1–13,19,20], and the other is freezable bound water lowering the freezing and melting temperature due to the polymer–water interaction [14–18]. As previously investigated with the PMMA membrane,

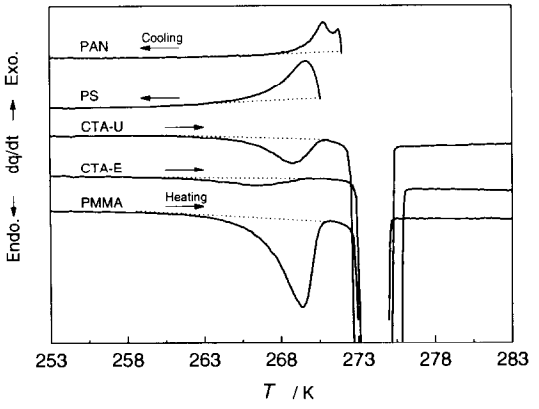

Fig. 1. DSC curves of the hydrogel-hollow-fiber membranes before freeze-drying.

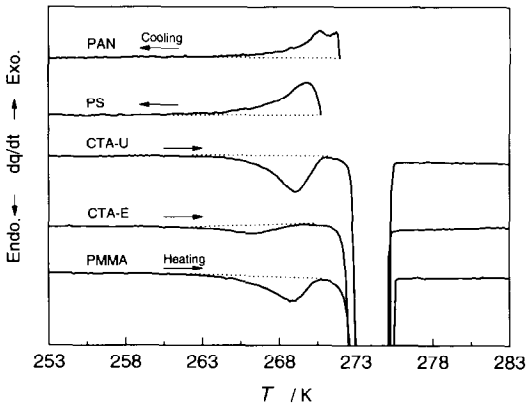

Fig. 2. DSC cooling curves of hydrogel-hollow-fiber membranes refilled with water after freeze-drying.

the freezing and melting depression water in a plate-like PMMA membrane was assigned to freezable pore water on the basis of the heat capacity of water [20] and the correlation time estimated from proton nuclear magnetic resonance [21]. Furthermore, considering the findings obtained by Homshaw regarding the water in non-dried PAN fibers, the water could also be assigned to freezable pore water. Accordingly, the PSD concerning the PMMA and PAN membranes can be determined from the distribution of the melting or freezing temperature of freezable pore water. On the contrary, for the CTA and PS membranes, it was obscure whether or not the melting or freezing temperature depression water was freezable pore water. Accordingly, based on the assumption that the water is pore water, the PSDs of CTA and PS were calculated from the distributions of the melting or freezing temperature of the water as described later.

Incidentally, the DSC curves of the membranes refilled with water after freeze-drying, i.e. after nitrogen gas adsorption-desorption, are shown in Fig. 2. By comparison of the DSC curves of the PMMA membrane shown in Figs. 1 and 2, the peak area of the DSC curve of the membrane after freeze-drying was found to be smaller than that of the membrane before freeze-drying. Furthermore, the peak area of the DSC curve of CTA-U after freeze-drying was slightly larger than that before freeze-drying, although the DSC curves of the other membranes were nearly similar before and after freeze-drying.

3.2. Pore size distribution curves of the membranes determined via thermoporosimetry and nitrogen gas adsorption-desorption

The PSD curves of the membranes before and after freeze-drying were determined from the DSC curves via thermoporosimetry. The concrete procedures for the calculation were described in detail in separate papers [11–13]. As previously reported [12,13], the freezing or melting depression ΔT is related to the pore radius R using the following equation:

$$R = \frac{\alpha(T)}{\Delta T} + \beta \tag{1}$$

where $\alpha(T)$ is a coefficient as a function of temperature which was determined to be $56.36\Delta T - 0.90$ during freezing and $33.30\Delta T - 0.32$ during melting in the case of a cylindrical pore [11]. The first term on the right side of the equation represents the radius of freezable pore water, while the second term, β, is the thickness of non-freezable pore water adsorbed on the surface of the pores. As reported earlier, the β values for silica gels were calculated by repetitive optimizations [11,12]; whereas it was difficult to determine the β values for PMMA membranes because the non-freezable water could exist not only on the pore surface but also in the PMMA matrix [26]. In general, two or three monolayers of adsorbed water on some materials have been reported in the literature [22–26], and hence the assumption that the β values in the membranes equal 1.0 nm, which corresponds to nearly three monolayers, would be reasonable. The error on the basis of the assumption may be negligible, so that it could be estimated to be less than about ±0.5 nm because a layer of non-freezable water of more than three molecules in thickness has not been reported so far in the literature.

Furthermore, the heat flow, dq/dt, of the DSC curve was converted into a derivative volume change in the pores using the following expression:

$$\frac{dV}{dR} = \frac{dq}{dt}\frac{dt}{dR}\frac{1}{m\Delta H(T)\rho_{fp}(T)}\frac{R^z}{(R-\beta)^Z} \tag{2}$$

where V is the cumulative pore volume as a function of the pore radius, m is the weight of the polymer, $\Delta H(T)$ is the enthalpy change in the phase transition of the freezable pore water, which was reasonably assumed to be the same as that of bulk water as a function of temperature, and $\rho_{fp}(T)$ is the density of the freezable pore water as a function of temperature. The $\rho_{fp}(T)$ can be approximated as the density of bulk ice during melting; it can also be approximated as the density of the supercooled water during freezing [26]. Moreover, z is a factor representing the shape of the pore which equals 2.0 for a cylindrical pore and 3.0 for a spherical pore. In the present work, the pore shape in the membranes was assumed to be cylindrical, viz. $z = 2.0$.

The PSDs calculated from the freezing or melting temperature distributions of the water in the membranes before and after freeze-drying using thermoporosimetry are shown by the solid and chain curves, respectively, in Figs. 3–8. In order to confirm the validity of the PSD curves, nitrogen gas adsorption-desorption measurements of the membranes that were prepared by freeze-drying were also carried out. Firstly, the nitrogen gas adsorption was carried out, and then the nitrogen gas desorption curve was measured. The PSD curves of the membranes were calculated from the nitrogen gas desorption curves using a technique established by Dollimore and Heal [27]. The closed circles in Figs. 3–7 represent the calculation results of the membranes after freeze-drying obtained using that technique.

As shown in Fig. 3, for the PMMA membrane after freeze-drying, the PSD curve obtained using nitrogen gas desorption was generally in good agreement with that obtained

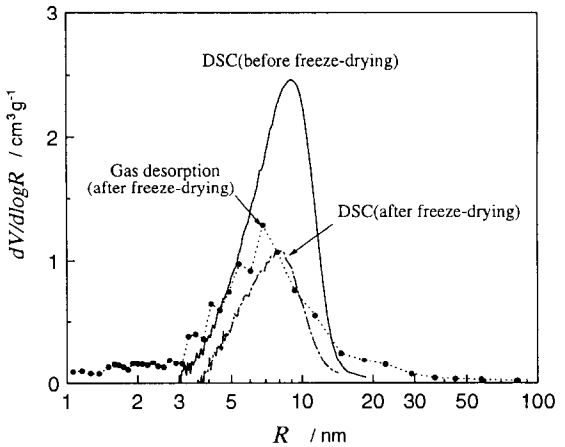

Fig. 3. Comparison of the PSD curves of the PMMA membrane determined via thermoporosimetry before (solid curve) and after (chain curve) freeze-drying with the PSD curve determined using the nitrogen gas desorption technique (closed circles).

via thermoporosimetry. Therefore, the PSDs determined via thermoporosimetry were concluded to be valid. As can been seen from Fig. 3, the PSD curves before and after freeze-drying were quite different. After freeze-drying, the peak radius of the PSD curve was shifted on the low radius side and the pore volume, viz. the peak area, was smaller than that before freeze-drying. Consequently, the pore structure of the PMMA membranes was concluded to be destroyed by the shrinkage due to freeze-drying. Probably, the change in the PSDs before and after freeze-drying may be proved for the first time

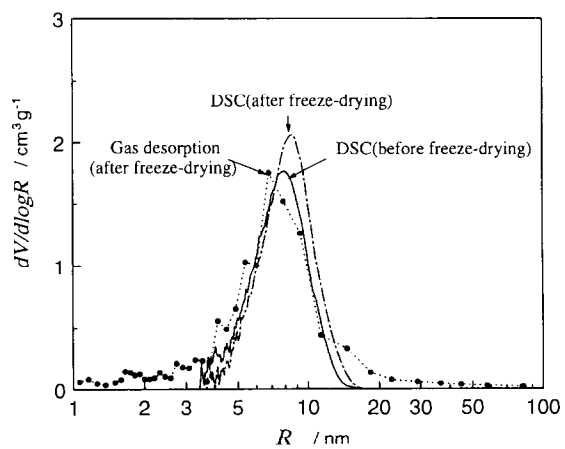

Fig. 4. Comparison of the PSD curves of the CTA-U membrane determined via thermoporosimetry before (solid curve) and after (chain curve) freeze-drying with the PSD curve determined using the nitrogen gas desorption technique (closed circles).

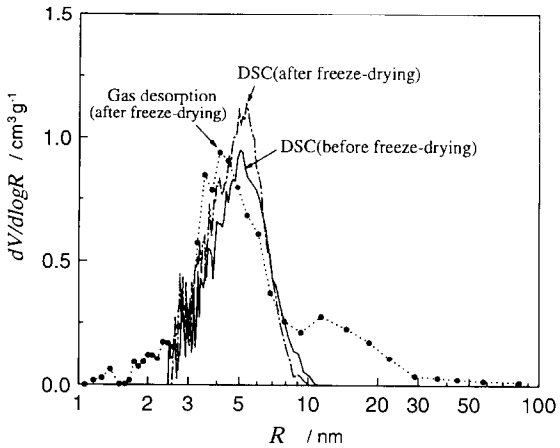

Fig. 5. Comparison of the PSD curves of the CTA-E membrane determined using thermoporosimetry before (solid curve) and after (chain curve) freeze-drying with the PSD curve determined using the nitrogen gas desorption technique (closed circles).

with regard to a polymer hydrogel system by means of thermoporosimetry, because the conventional technique for the pore analysis cannot be applied to wet materials. Applicability to wet materials without drying is the advantage of thermoporosimetry.

In contrast, for CTA-U and CTA-E as shown in Figs. 4 and 5, the PSD curves after freeze-drying obtained via nitrogen gas desorption were generally in good agreement with those of the membranes before and after freeze-drying determined via thermoporosimetry, though the PSD curves after freeze-drying were slightly larger than those be-

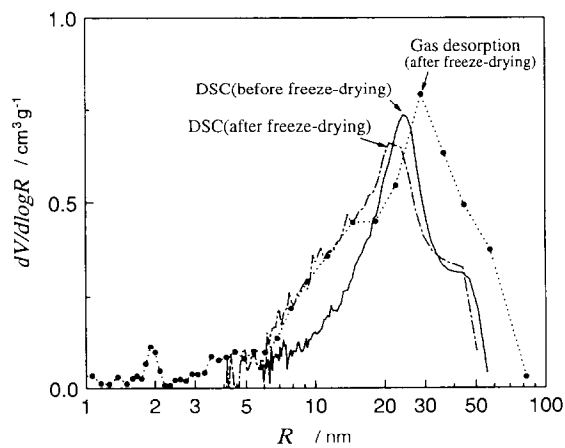

Fig. 6. Comparison of the PSD curves of the PAN membrane determined using thermoporosimetry before (solid curve) and after (chain curve) freeze-drying with the PSD curve determined using the nitrogen gas desorption technique (closed circles).

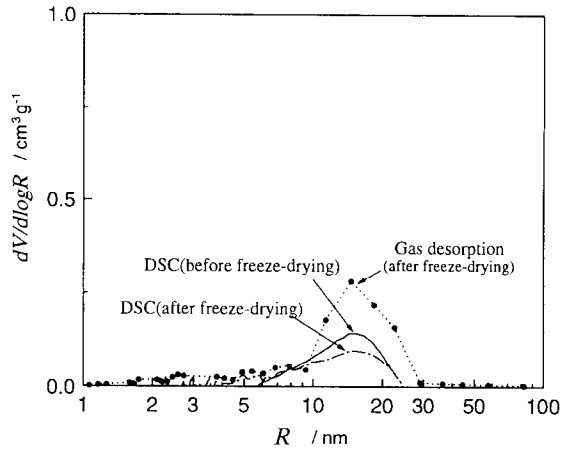

Fig. 7. Comparison of the PSD curves of the PS membrane determined via thermoporosimetry before (solid curve) and after (chain curve) freeze-drying with the PSD curve determined using the nitrogen gas desorption technique (closed circles).

fore freeze-drying. This slight enlargement of the pore volume after freeze-drying in both membranes may be related to the destruction of the pore structure due to the freezing of water by liquid nitrogen.

According to scanning electron micrographs (SEM) of the PS and PAN membranes, a thin activated layer, which would be relevant to the permeation of water and solute through the membranes, was on the top surface on one side of both membranes. The average pore size of the supporting layer was much larger than that of the activated layer. Although it is impossible to determine only the PSD of the activated layer on the surface because the pore volume was rather small, the overall PSDs of the membranes can be

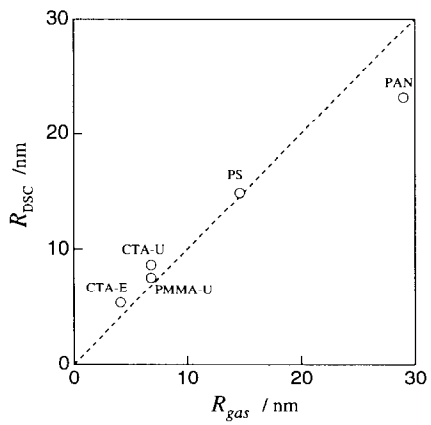

Fig. 8. Comparison of the peak radii of the PSD curves in the membranes after freeze-drying determined via thermoporosimetry and the nitrogen gas desorption technique.

determined via thermoporosimetry and nitrogen gas desorption. The calculation results are given in Figs. 6 and 7. For the PAN membrane as shown in Fig. 6, the peak radius obtained using nitrogen gas adsorption-desorption was generally consistent with those obtained via thermoporosimetry regarding the membranes before and after freeze-drying, suggesting that the pore structure of PAN is likely not destroyed by freeze-drying. Similar findings were obtained in the PS membrane. As can been seen from Fig. 7, the peak radius of the PSD curve obtained using nitrogen gas desorption was generally consistent with those obtained via thermoporosimetry regarding the PS membranes before and after freeze-drying.

3.4. Pore structural properties calculated from the PSD curves

The peak radii, R_{DSC}, of the PSD curves, the pore volumes, V_{DSC}, and the specific surface areas, S_{DSC}, of the membranes before freeze-drying, which were calculated from the PSD curves determined using the previously reported procedure [12] via thermoporosimetry, are summarized in Table 1. The geometric average pore radii, R_{34}, of three order and four order average radii defined in the previous paper [13], which are related to the permeability of water through the membranes in the case of symmetrically cylindrical pores [28], are also listed in the table. In the present paper, the water permeabilities of the membranes were also measured, and then the average pore radii of the PMMA, CTA-U and CTA-E membranes were hydrodynamically determined to be 7.8, 7.2 and 4.7 nm, respectively. The values were reasonably consistent with the R_{34} values in Table 1.

Furthermore, the peak radii, R_{DSC} and R_{gas}, and the pore volumes, V_{DSC} and V_{gas}, in the membranes after freeze-drying were calculated from the PSD curves determined via thermoporosimetry and nitrogen gas desorption, respectively, as summarized in Table 2.

The relationship between the R_{DSC} and the R_{gas} in the membranes after freeze-drying is graphically shown in Fig. 8. The plots are linear, and hence the experimental results obtained using both techniques are consistent. In addition, Fig. 9 illustrates the comparison of the pore volumes in the membranes after freeze-drying determined using both techniques. The V_{DSC} values are found to correlate with the V_{gas} values. Consequently, although the theoretical and experimental backgrounds are quite different with respect to thermoporosimetry and nitrogen gas adsorption-desorption, the pore radii and the pore volumes in the membranes after freeze-drying were consistent in both techniques. Con-

Table 1
The pore structures of the membranes before freeze-drying determined using DSC curves

Sample	R_{DSC} /nm	V_{DSC} /cm^3 g^{-1}	S_{DSC} /m^2 g^{-1}	R_{34} /nm
PMMA	8.1	0.758	202.5	8.0
CTA-U	8.1	0.513	143.8	8.0
CTA-E	4.8	0.309	129.2	5.5
PAN	24.6	0.317	32.6	27.0
PS	15.5	0.049	6.3	15.0

Table 2

Comparison of the pore structures determined using DSC with those obtained via nitrogen gas adsorption-desorption for the membranes after freeze-drying

Sample	DSC		Nitrogen gas	
	R_{DSC} /nm	V_{DSC} /cm^3 g^{-1}	R_{gas} /nm	V_{gas} /cm^3 g^{-1}
PMMA	7.5	0.3105	6.8	0.6007
CTA-U	8.6	0.5658	6.8	0.6522
CTA-E	5.3	0.3181	4.1	0.4287
PAN	23.2	0.3840	29.0	0.5120
PS	14.9	0.0428	14.6	0.1230

sidering the findings, the assumption that the freezing or melting depression water in the PMMA, CTA, PAN, PS membranes is freezable pore water must be justified. Thermoporosimetry is concluded to be an available technique for precisely determining the PSDs of polymer hydrogel membranes without freeze-drying.

4. Conclusion

The pore size distributions of the hydrogel-hollow-fiber membranes, such as poly(methyl methacrylate), cellulose triacetate, polysulfone and polyacrylonitrile for artificial kidneys, were determined using thermoporosimetry and nitrogen gas adsorption-desorption. For the membranes after freeze-drying, the pore size distributions obtained using nitrogen gas desorption were found to be generally in good agreement with those

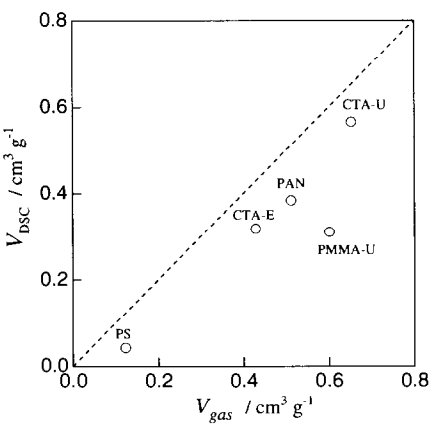

Fig. 9. Comparison of the pore volume of the PSD curves in the membranes after freeze-drying determined via thermoporosimetry and the nitrogen gas desorption technique.

obtained using thermoporosimetry regarding the membranes refilled with water after freeze-drying. Consequently, it was concluded that the PSDs of the membranes determined via thermoporosimetry were justified and that the freezing and melting depression of water in the membranes was assigned to freezable pore water. Furthermore, the PSDs of the poly (methyl methacrylate) hydrogel membrane before and after freeze-drying were found to be quite different, and hence the pore structures were proved to be destroyed by freeze-drying.

References

[1] L.G. Homshaw, J. Colloid Interface Sci., 84 (1981) 127.
[2] C. Eyraud, Themochim. Acta, 100 (1986) 223.
[3] M. Brun, A. Lallemand, J.F. Quinson and C. Eyraud, Themochim. Acta, 21 (1977) 59.
[4] M. Brun, J.F. Quinson and L. Benoist, Themochim. Acta, 49 (1981) 49.
[5] J.F. Quinson, J. Dumas and J. Serughetti, J. Non-Cryst. Solids, 79 (1986) 397.
[6] J.F. Quinson, Appl. Catal., 30 (1987) 123.
[7] E. Françoise and L. Jacques, Colloids Surf., 23 (1987) 105.
[8] L. Zeman, G. Tkacik and P. Le Parlouer, J. Membr. Sci., 32 (1987) 329.
[9] F. Ehrburger-Dolle, S. Misono and J. Lahaye, J. Colloid Interface Sci., 35 (1990) 468.
[10] F. Ehrburger and J. Lahaye, J. Colloids Surf., 23 (1987) 105.
[11] K. Ishikiriyama, M. Todoki and K. Motomura, J. Colloid Interface Sci., 171 (1995) 92.
[12] K. Ishikiriyama and M. Todoki, J. Colloid Interface Sci., 171 (1995) 103.
[13] K. Ishikiriyama, M. Todoki, T. Kobayashi and H. Tanzawa, J. Colloid Interface Sci., 173 (1995) 419.
[14] A. Higuchi and T. Iijima, Polymer, 26 (1984) 1833.
[15] K. Nakamura, T. Hatakeyama and H. Hatakeyama, Polymer, 24 (1983) 871.
[16] K. Nakamura, T. Hatakeyama and H. Hatakeyama, Text. Res. J., 51 (1981) 607.
[17] Y. Taniguchi and S. Horigome, J. Appl. Polym. Sci., 19 (1975) 2743.
[18] T. Hatakeyama, K. Nakamura and H. Hatakeyama, Thermochim. Acta, 123 (1988) 153.
[19] H.G. Burghoff and W. Push, J. Appl. Polym. Sci., 23 (1979) 473.
[20] K. Ishikiriyama and M. Todoki, J. Polym. Sci., Part B Polym. Phys., 33 (1995) 791.
[21] A. Yamada-Nosaka, K. Ishikiriyama, M. Todoki and H. Tanzawa, J. Appl. Polym. Sci., 39 (1990) 2443.
[22] Y. P. Handa, M. Zakrzewski and C. Fairbridge, J. Phys. Chem., 96 (1992) 8594.
[23] W. Drost-Hansen, Ind. Eng. Chem., 61 (1969) 10.
[24] A.A. Antoniu, J. Phys. Chem., 68 (1964) 2745.
[25] G.G. Litvan, Can. J. Chem., 44 (1966) 2617.
[26] K. Ishikiriyama and M. Todoki, Thermochim. Acta, 256 (1995) 213.
[27] D. Dollimore and G.R. Heal, J. Appl. Chem., 14 (1964) 109.
[28] K. Kamide, S. Manabe and T. Matsui, Koubunshi Ronbunsyu, 34 (1977) 2.